網膜血管新生抑制機構の解明とその応用に関する研究

厚生労働科学研究研究費補助金　感覚器障害研究事業
平成16年度　総括・分担研究報告書

平成17年３月

主任研究者　細谷　健一

目　次

厚生労働科学研究費補助金（感覚器障害研究事業）
総括研究報告書

網膜ペリサイト由来の網膜血管内皮細胞増殖抑制因子の同定

主任研究者　細谷　健一　富山医科薬科大学・薬学部　教授

研究要旨：本研究は網膜ペリサイト由来の網膜血管内皮細胞の増殖抑制因子を同定することを目的とした。独自に樹立した網膜ペリサイト株(TR-rPCT)培養濃縮液からタンパクの分子量および荷電によりフラクションを分け、内皮細胞増殖抑制効果から指標タンパクとした。質量分析法を用いて、網膜毛細血管内皮細胞増殖抑制因子の１つの候補として新規トロポミオシンを同定し、大腸菌を用いてリコンビナント体を作製した。新規トロポミオシンの網膜毛細血管内皮細胞増殖抑制効果の 50%阻害濃度は約２μM であった。以上の結果から、網膜ペリサイト由来の網膜血管内皮細胞増殖抑制因子の有力候補の１つが同定できた。

分担研究者　登美　斉俊　富山医科薬科大学・薬学部　助手
分担研究者　笹岡　利安　富山医科薬科大学・薬学研究科　助教授

A．研究目的

糖尿病網膜症、未熟児網膜症などの網膜における血管新生は、網膜毛細血管の周囲にあるペリサイトの脱落から始まっている。我々は網膜ペリサイトから分泌される因子が網膜毛細血管内皮細胞の増殖を制御していると仮説を立て、我々が樹立した網膜毛細血管内皮細胞株(TR-iBRB)と網膜ペリサイト株(TR-rPCT)の共培養解析の結果、TR-rPCT 細胞培養後の培地の濃縮液を TR-iBRB 細胞に添加すると増殖が著しく抑制されることを見いだした。網膜ペリサイト株から分泌される細胞増殖抑制因子を同定することは糖尿病網膜症の治療への応用、または発症のメカニズム解明と新しい学問の突破口となる可能性が高く社会的にも重要である。

そこで本研究では、網膜ペリサイトから分泌される網膜血管内皮細胞増殖因子を同定することを目的とした。

B．研究方法

TR-rPCT 細胞を Dulbecco's modified Eagle's medium (DMEM)で培養し、培養濃縮液は培養液上清を限外濾過法によって調製した。培養濃縮液からのタンパク精製は、硫安沈殿させたタンパクを陰イオン交換クロマトグラフィー、ハイドロキシアパタイトクロマトグラフィーでフラクションに分離した。各フラクションの細胞増殖抑制効果は TR-iBRB 細胞における 5-bromo-2'-deoxyuridine(BrdU)の取り込みによる DNA 合成活性から判定した。細胞増殖抑制効果の高いフラクションを二次元電気泳動で分離後、マトリックス支援レ

ーザー脱離イオン化飛行時間型質量分析装置（MALDI-TOFMS）で質量ならびにアミノ酸配列を解析した。さらに、Peptide Mass Fingerprinting (PMF)解析、データベース（GenBank）を活用し、全アミノ酸配列を決定した。

C．研究結果

TR-rPCT 細胞の培養濃縮液タンパクは60のフラクションに分離した。60のフラクションの中でNo. 25のフラクション付近でBrdU の強い取り込み抑制が示された。このフラクションタンパクを2次元電気泳動にて分離し、MALDI-TOFMS、PMF 解析からトロポミオシン(TM)であることが示唆された。この TM タンパクは、今までに報告されている TM3、TM6 および TMαと相同性が高いものの、これらとは一致しない配列であった。ラット TM3、TM6 を特異的に認識するプライマーを用いてPT-PCR 法でオープンリーディングフレーム（ORF）のクローニングを行った。その結果、ラット網膜および TR-rPCT 細胞に新規に単離したタンパクをコードするmRNA が発現していることが示された。増幅された PCR 産物の遺伝子配列から予想されるアミノ酸配列からも TM3、TM6 および TMαとは異なるタンパクであることが示唆された。

新規に単離された TM タンパクのリコンビナント体を作製するために、目的遺伝子の ORF を発現誘導ベクターに導入し、大腸菌にて大量に培養した。タンパクは大腸菌から収集、精製した。精製したタンパクはMALDI-TOFMS によってタンパク質量を、プロテインシークエンサーを用いてN末端アミノ酸配列解析を行い単離したタンパクと同一であることを確認した。

得られたタンパクの内皮細胞増殖抑制効果は、TR-iBRB 細胞を用いて解析した。TR-rPCT 細胞の5倍培養濃縮液をコントロールにして測定したところ、新規に単離したTMタンパクは濃度依存的にTR-iBRB細胞の増殖を抑制し、50%阻害濃度は約 2 μM であった。一方、ウシ血清アルブミンを添加した場合、細胞増殖抑制効果は示されなかったことから、新規に単離した TM タンパクの内皮細胞増殖抑制効果は特異的であることが示唆された。

D．考察

TR-rPCT 細胞培養濃縮液から TR-iBRB 細胞増殖抑制効果を示すタンパクとして新規 TM を単離した。このタンパクは TR-rPCT、ラット網膜に発現していることが示され、TR-iBRB 細胞の増殖抑制効果を示したことから、in vivo においても細胞増殖抑制に関与している可能性がある。今後、内皮細胞増殖抑制メカニズム、効果発現の様式を研究することで糖尿病網膜症治療薬として開発につながるものと思われる。

E．結論

本研究によって、網膜ペリサイトから分泌される網膜血管内皮細胞増殖因子の1つとして新規トロポミオシンの関与を明らかにした。物質の同定のみならず、タンパクのリコンビナント体を作製にも成功した。今後は、このタンパクの内皮細胞増殖抑制メカニズムを解明し、薬理効果を証明する予定である。

F．健康危険情報

特になし

G．研究発表

1．論文発表

Hosoya K, Minamizono A, Katayama K, Terasaki T, Tomi M., Vitamin C transport in oxidized form across the rat blood-retinal barrier. *Invest Ophthalmol Vis Sci.* 45, 1232-1239 (2004).

Sasaoka T, Wada T, Fukui K, Murakami S, Ishihara H, Suzuki R, Tobe K, Kadowaki T, Kobayashi M., SH2-containing inositol phosphatase 2 predominantly regulates Akt2, and not Akt1, phosphorylation at the plasma membrane in response to insulin in 3T3-L1 adipocytes. *J Biol Chem.* 279, 14835-14843 (2004).

Nakashima T, Tomi M, Katayama K, Tachikawa M, Watanabe M, Terasaki T, Hosoya K., Blood-to-retina transport of creatine via creatine transporter (CRT) at the rat inner blood-retinal barrier. *J Neurochem.* 89, 1454-1461 (2004).

Tomi M, Abukawa H, Nagai Y, Hata T, Takanaga H, Ohtsuki S, Terasaki T, Hosoya K., Retinal selectivity of gene expression in rat retinal versus brain capillary endothelial cell lines by differential display analysis. *Mol Vis.* 10, 537-543 (2004).

Fernandes R, Carvalho AL, Kumagai A, Seica R, Hosoya K, Terasaki T, Murta J, Pereira P, Faro C., Downregulation of retinal GLUT1 in diabetes by ubiquitinylation. *Mol Vis.* 10, 618-628 (2004).

Tomi M, Hosoya K., Application of magnetically isolated rat retinal vascular endothelial cells for the determination of transporter gene expression levels at the inner blood-retinal barrier. *J Neurochem.* 91, 1244-1248 (2004).

Hosoya K, Tomi M., Advances in the cell biology of transport via the inner blood-retinal barrier: establishment of cell lines and transport functions. *Biol Pharm Bull.* 28, 1-8 (2005).

2．学会発表

Hosoya K, Nakashima T, Katayama K, Tachikawa M, Watanabe M, Terasaki T, Tomi M., CRT as a system responsible for the transport of creatine at the inner blood-retinal barrier, The Association of Research in Vision and Ophthalmolgy, May 2004, Fort Lauderdale USA.

Leal EC, Aveleira C, Sa M, Serra A, Castilho A, Terasaki T, Hosoya K, Cunha-Vaz J, Ambrosio AF. Rat retinal endothelial cell dysfunction induced by

hyperglycemia and oxidative stress: additive effects? The Association of Research in Vision and Ophthalmolgy, May 2004, Fort Lauderdale USA.

Fernandes R, Carvalho AL, Kumagai AK, Seica R, Hosoya K, Terasaki T, Murta J, Pereira P, Faro C. Downregulation of retinal GLUT1 in diabetes by the ubiquitin proteasome pathway. The Association of Research in Vision and Ophthalmolgy, May 2004, Fort Lauderdale USA.

Tomi M, Minamizono A, Hosoya K. Magnetically isolation and characterization of rat retinal vascular endothelial cells (RVEC), 2nd Pharmaceutical Science World Congress, May 2004, Kyoto.

Hosoya K, Tomi M. Retinal vascular endothelial cell purification method for the determination of mRNA expression at the inner blood-retinal barrier, AAPS annual meeting and exposition, November 2004, Baltimore USA.

H．知的財産権の出願・登録情報

１．特許取得　特願 2005-62066

発明者：細谷健一、寺崎哲也、大槻純男、登美斉俊、特許出願人：国立大学法人富山医科薬科大学　代表　小野武年、発明の名称：網膜周皮細胞由来の細胞増殖抑制因子

２．実用新案登録　なし

３．その他　なし

厚生労働科学研究費補助金（感覚器障害研究事業）
分担研究報告書

網膜ペリサイト由来液性因子による PKC/MAPK 系を介した網膜血管内皮細胞増殖抑制

分担研究者　寺崎　哲也　東北大学未来科学技術共同研究センター　教授

研究要旨：本研究は網膜ペリサイト由来液性因子による網膜血管内皮細胞の増殖抑制シグナル伝達機構を解析することを目的とした。独自に樹立した網膜ペリサイト株(TR-rPCT)の conditioned medium (rPCT-CM)は網膜毛細血管内皮細胞株(TR-iBRB)の増殖、DNA 合成量を濃度依存的に減少させることが示された。TR-iBRB 細胞における G1 期から S 期への移行を促進する cyclin D1、cyclin-dependent kinase 4 (cdk4)、および cdk6 の発現は、rPCT-CM 添加によって減少した。Protein kinase C (PKC) α/βII および p44/22 mitogen-activated protein kinase (MAPK)の活性化は rPCT-CM 添加によって阻害された。さらに、虚血誘導性網膜症マウスにおける in vivo 網膜血管新生は rPCT-CM 添加によって阻害された。以上の結果から、網膜ペリサイト由来液性因子は p44/22 MAPK の抑制を通して内皮細胞の増殖を抑制し、網膜血管新生を阻害することが示唆された。

A．研究目的

糖尿病網膜症の初期において網膜毛細血管内皮細胞を取り囲んでいるペリサイトが選択的に脱落して既存の毛細血管内皮細胞が増殖し、血管新生が生じる。このことから、網膜ペリサイトが血管の異常増殖を抑制していると考えられてきた。しかし、網膜ペリサイトの網膜内皮細胞に対する増殖抑制機序には不明な点が多く残っている。

細胞増殖機構の研究には培養細胞が多く用いられている。しかし、網膜は微小組織のため、網膜内皮細胞やペリサイトの初代培養細胞は大量に調製しにくい。我々は近年、温度感受性 SV40 T 抗原遺伝子導入トランスジェニックラットから網膜毛細血管内皮細胞株(TR-iBRB)および網膜ペリサイト株(TR-rPCT)を樹立した。そこで本研究では TR-rPCT 細胞の conditioned medium (rPCT-CM)を用いて網膜血管新生の抑制機序を in vitro で解析し、さらに虚血誘導性網膜症マウスに rPCT-CM を投与することで in vivo における血管新生抑制効果を検討することを目的とした。

B．研究方法

rPCT-CM は TR-rPCT 細胞培養上清を限外濾過法によって濃縮した。TR-iBRB 細胞における細胞周期制御タンパクおよび増殖シグナルタンパクの発現変動は、10% FBS Dulbecco's modified Eagle's medium (DMEM)で培養した条件と 10% FBS rPCT-CM で培養した条件を比較検討した。DNA 合成量は 5-bromo-2'-deoxy-uridine (BrdU)の DNA への取り込みを ELISA 法に

より定量した。In vivo での網膜血管新生抑制効果は、虚血誘導性網膜症マウスを用いた。生後 7 日目(P7)から P12 まで 75%酸素下で飼育後 P12 から 5 日間 PBS または rPCT-CM を投与したマウスに対し、P17 に心臓から FITC-dextran を灌流することで網膜血管を可視化して評価した。

C．研究結果

ペリサイトの液性因子が内皮細胞に対して及ぼす影響を解析するために、rPCT-CM を TR-iBRB 細胞に添加した結果、TR-iBRB 細胞の増殖は rPCT-CM の濃度依存的に抑制された。ヒト臍帯静脈内皮細胞およびヒト脳毛細血管内皮細胞の増殖についても 5 倍濃縮 rPCT-CM 添加で抑制された一方、T 抗原遺伝子導入不死化細胞株 COS7 の増殖には影響を与えなかった。5 倍濃縮 rPCT-CM 添加時の TR-iBRB 細胞における細胞周期制御タンパクへの影響を Western blot 法によって解析した。その結果、cyclin D1、cyclin-dependent kinase 4 (cdk4)、cdk6 の発現は 5 倍濃縮 rPCT-CM を添加することで減少した。DNA-polymerase-δ associated protein である proliferating cell number antigen (PCNA)の発現も 5 倍濃縮 rPCT-CM を添加した TR-iBRB 細胞において減少する傾向を示した。さらに、TR-iBRB 細胞における BrdU の取り込み量を測定したところ、rPCT1-CM の濃度依存的に BrdU 取り込みが減少し、DNA 合成が抑制されていることが示された。

細胞増殖は細胞外からの増殖促進因子の刺激によって誘導される。そこで rPCT1-CM が FBS による増殖促進シグナルを抑制するかどうかを Western blot 法によって検討した。TR-iBRB 細胞に 10% FBS DMEM を添加したところ、protein kinase C (PKC) α/βII および p44/22 mitogen-activated protein kinase (MAPK) が活性化された。しかし、10% FBS を含む 5 倍濃縮 rPCT-CM を添加すると、PKC α/βII および p44/22 MAPK のリン酸化体が短時間で減少する傾向を示した。一方、protein kinase B (Akt)は 10% FBS DMEM を添加してもリン酸化体はほとんど検出されず、10% FBS を含む 5 倍濃縮 rPCT-CM によっても活性化されなかった。

rPCT-CM の細胞増殖抑制効果を in vivo で評価するために、虚血誘導性網膜症マウスを用いた。虚血誘導性網膜症マウスに対して FITC-dextran を投与したところ、網膜血管からの FITC-dextran の漏出が示された。一方、rPCT-CM 50 μg を 24 時間間隔で投与した虚血誘導性網膜症マウスでは、網膜血管からの FITC-dextran の漏出が減少した。

D．考察

rPCT-CM は網膜血管内皮細胞を含む内皮細胞の増殖抑制効果を有していることから、rPCT-CM には内皮細胞の増殖を抑制する液性因子が存在することが示唆された。さらに、rPCT-CM を添加した TR-iBRB 細胞において、G1 期から S 期への移行を促進する cyclin D1、cdk4、および cdk6 の発現および DNA 合成が減少し、PKC および p44/22 MAPK の増殖シグナル経路が抑制されていることが示された。網膜血管新生機序では PKCβII 介在型 p44/22 MAPK が活性化されることで、内皮細胞の増殖が促進されることが報告されている。さらに、

このシグナリングは糖尿病網膜症時の血管新生への関与も報告されている。したがって、rPCT-CMはTR-iBRB細胞の増殖シグナル経路PKC介在型p44/22 MAPKを抑制し、その下流のcyclin D、cdk4/6の発現を減少させることで細胞周期をG1/S期で抑制していることが示唆された。

虚血誘導性網膜症マウスにおいてFITC-dextran漏出が示されたことから、本マウスにおいてバリアー機能が著しく低下した血管の新生が生じ、FITC-dextranが内皮細胞の間隙から漏れ出てきたと考えられる。一方、rPCT-CMの投与によってFITC-dextran漏出の減少が示され、rPCT-CMは虚血誘導性網膜血管新生を阻害することが示された。本結果から、rPCT-CM中には単にin vitroで内皮細胞の増殖性を低下させる因子が存在するだけでなく、in vivoにおいても網膜血管新生の阻害に有効な因子を含んでいることが示唆された。

E．結論

本研究によって、網膜ペリサイト液性因子がPKC介在型p44/22 MAPKシグナリングを抑制することによって網膜血管新生を阻害することを明らかにした。現在、世界中で糖尿病に罹る人が増加するにつれて、後天性の失明も増加している。ペリサイト液性因子には視覚障害から患者を守ることができる重要な因子が存在する可能性がある。

F．健康危険情報

特になし

G．研究発表

1．論文発表

Hori S, Ohtsuki S, Hosoya K, Nakashima E, Terasaki T. A pericyte-derived angiopoietin-1 multimeric complex induces occludin gene expression in brain capillary endothelial cells through Tie-2 activation in vitro. *J Neurochem* 89, 503-513 (2004).

Hori S, Ohtsuki S, Tachikawa M, Kimura N, Kondo T, Watanabe M, Emi Nakashima, Terasaki T. Functional expression of rat ABCG2 on the luminal side of brain capillaries and its enhancement by astrocyte-derived soluble factor(s). *J Neurochem* 90, 526-536 (2004).

Kondo T, Hosoya K, Hori S, Tomi M, Ohtsuki S, Terasaki T. PKC/MAPK signaling suppression by retinal pericyte conditioned medium prevents retinal endothelial cell proliferation. *J Cell Physiol* 203, 378-386 (2005).

2．学会発表

なし

H．知的財産権の出願・登録情報

1．特許取得　なし

2．実用新案登録　なし

3．その他

研究成果の刊行に関する一覧表

発表者氏名	論文タイトル名	発表誌名	巻号	ページ	出版年
Hosoya K, Minamizono A, Katayama K, Terasaki T, Tomi M.,	Vitamin C transport in oxidized form across the rat blood-retinal barrier.	Invest Ophthalmol Vis Sci	45	1232-1239	2004
Sasaoka T, Wada T, Fukui K, Murakami S, Ishihara H, Suzuki R, Tobe K, Kadowaki T, Kobayashi M.	SH2-containing inositol phosphatase 2 predominantly regulates Akt2, and not Akt1, phosphorylation at the plasma membrane in response to insulin in 3T3-L1 adipocytes.	J Biol Chem	279	14835-14843	2004
Nakashima T, Tomi M, Katayama K, Tachikawa M, Watanabe M, Terasaki T, Hosoya K.	Blood-to-retina transport of creatine via creatine transporter (CRT) at the rat inner blood-retinal barrier.	J Neurochem	89	1454-1461	2004
Tomi M, Abukawa H, Nagai Y, Hata T, Takanaga H, Ohtsuki S, Terasaki T, Hosoya K.	Retinal selectivity of gene expression in rat retinal versus brain capillary endothelial cell lines by differential display analysis.	Mol Vis	10	537-543	2004
Fernandes R, Carvalho AL, Kumagai A, Seica R, Hosoya K, Terasaki T, Murta J, Pereira P, Faro C.	Downregulation of retinal GLUT1 in diabetes by ubiquitinylation.	Mol Vis	10	618-628	2004
Tomi M, Hosoya K.	Application of magnetically isolated rat retinal vascular endothelial cells for the determination of transporter gene expression levels at the inner blood-retinal barrier.	J Neurochem	91	1244-1248	2004
Hosoya K, Tomi M.	Advances in the cell biology of transport via the inner blood-retinal barrier: establishment of cell lines and transport functions.	Biol Pharm Bull	28	1-8	2005
Hori S, Ohtsuki S, Hosoya K, Nakashima E, Terasaki T.	A pericyte-derived angiopoietin-1 multimeric complex induces occludin gene expression in brain capillary endothelial cells through Tie-2 activation in vitro.	J Neurochem	89	503-513	2004

Hori S, Ohtsuki S, Tachikawa M, Kimura N, Kondo T, Watanabe M, Emi Nakashima, Terasaki T.	Functional expression of rat ABCG2 on the luminal side of brain capillaries and its enhancement by astrocyte-derived soluble factor(s).	J Neurochem	90	526-536	2004
Kondo T, Hosoya K, Hori S, Tomi M, Ohtsuki S, Terasaki T.	PKC/MAPK signaling suppression by retinal pericyte conditioned medium prevents retinal endothelial cell proliferation.	J Cell Physiol	203	378-386	2005

Vitamin C Transport in Oxidized Form across the Rat Blood–Retinal Barrier

Ken-ichi Hosoya,[1,2] *Akito Minamizono,*[1] *Kazunori Katayama,*[1] *Tetsuya Terasaki,*[2-4] *and Masatoshi Tomi*[1,2]

PURPOSE. To elucidate the mechanisms of vitamin C transport across the blood–retinal barrier (BRB) in vivo and in vitro.

METHODS. [^{14}C]Dehydroascorbic acid (DHA) and [^{14}C]ascorbic acid (AA) transport in the retina across the BRB were examined using in vivo integration plot analysis in rats, and the transport mechanism was characterized using a conditionally immortalized rat retinal capillary endothelial cell line (TR-iBRB2) as an in vitro model of the inner BRB.

RESULTS. The apparent influx permeability clearance (K_{in}) per gram of retina of [^{14}C]DHA and [^{14}C]AA was found to be 2.44×10^{-3} μL/(min · g retina) and 65.4 μL/(min · g retina), respectively. In the retina and brain, the K_{in} of [^{14}C]DHA was approximately 38 times greater than that of [^{14}C]AA, whereas there was no major difference in the heart. The K_{in} of [^{14}C]DHA in the retina was eight times greater than that in the brain. HPLC analysis revealed that most of the vitamin C accumulated in AA form in the retina. These results suggest that vitamin C is mainly transported in DHA form across the BRB and accumulates in AA form in the rat retina. In an in vitro uptake study in TR-iBRB2 cells, the initial uptake rate of [^{14}C]DHA was 37 times greater than that of [^{14}C]AA, which is in agreement with the results of the in vivo study. [^{14}C]DHA uptake by TR-iBRB2 cells took place in an Na^+-independent and concentration-dependent manner with a K_m of 93.4 μM. This process was inhibited by substrates and inhibitors of glucose transporters. [^{14}C]DHA uptake was inhibited by D-glucose in a concentration-dependent manner with a 50% inhibition concentration of 5.56 mM. Quantitative real-time PCR and immunostaining analyses revealed that expression of GLUT1 and -3 was greater than that of the Na^+-dependent L-ascorbic acid transporter (SVCT)-2 in TR-iBRB2 cells.

CONCLUSIONS. Vitamin C is mainly transported across the BRB as DHA mediated through facilitative glucose transporters and accumulates as AA in the rat retina. (*Invest Ophthalmol Vis Sci.* 2004;45:1232–1239) DOI:10.1167/iovs.03-0505

Vitamin C, which is an essential substance in humans, acts as a cofactor in the enzymatic biosynthesis of collagen, catecholamine, and peptide neurohormones and as an antioxidant and/or free radical scavenger to detoxify free radicals in body tissues.[1] The retina is the only tissue in which light is focused on a group of cells. It is necessary to protect the retina against oxidative stress because light causes free radical oxidation.[2] Vitamin C is present in the retina at a high concentration compared with its presence in other organs in humans.[1,3] The concentration of L-ascorbic acid (AA) is approximately 1.6 mM in the rat and guinea pig retina, although the plasma concentration in most mammals is 50 to 100 μM,[3,4] suggesting that AA is transported from the circulating blood to the retina across the blood–retinal barrier (BRB) through a specific transport process. Possible sources of oxidative stress in diabetes and retinal diseases include increased generation of reactive oxygen species by autooxidation of D-glucose and a reduced tissue concentration of antioxidants.[5,6] It is important to elucidate the transport mechanisms for vitamin C as far as the supply of antioxidants in the neural retina is concerned.

The BRB, which is composed of retinal capillary endothelial cells (inner BRB) and retinal pigmented epithelial cells (RPE, outer BRB), plays a key role in restricting the nonspecific transport of hydrophilic compounds and facilitating the influx and efflux transport of essential molecules and xenobiotics, respectively, from the circulating blood to the retina and vice versa.[7,8] Na^+-dependent L-ascorbic acid transporter (SVCT)-1 and -2 have been cloned and mediate concentrated, high-affinity AA transport that is driven by the Na^+ electrochemical gradient.[9] Although SVCT2 mRNA is present in the retina,[9] its localization and transport functions are not fully understood. An Na^+-dependent L-ascorbic acid transport process and SVCT2 are present in RPE[10] and lens epithelial cells,[11] respectively. However, the Na^+-dependent L-ascorbic acid transport process in RPE is inhibited by D-glucose, suggesting that it may not be SVCT1 or -2.[10] The facilitative glucose transporters, GLUT1 and -3 mediate equilibrative and relatively low-affinity dehydroascorbic acid (DHA) transport.[12,13] DHA is an oxidized form of AA, and its plasma concentration is reported to be approximately 10 μM in the rat[14] and human.[15] Agus et al.[16] have reported that DHA crosses the blood–brain barrier (BBB) through GLUT1 at the luminal and abluminal side of BBB and accumulates as reduced AA in the brain. Although GLUT1 is expressed at both the inner BRB and RPE and plays an essential role in supplying D-glucose as an energy source in the neural retina,[17,18] our knowledge of vitamin C transport mechanism across the BRB is incomplete.

The purpose of this study was to elucidate the mechanisms of vitamin C transport across the BRB. To be able to understand the physiological and pathophysiological roles of BRB transport, we wanted to discover whether SVCT2 or glucose transporters make the greatest contribution to the supply of vitamin C to the retina.

From the [1]Faculty of Pharmaceutical Sciences, Toyama Medical and Pharmaceutical University, Toyama, Japan; [2]Core Research for Evolutional Science and Technology (CREST), Japan Science and Technology Corp., Japan; the [3]Department of Molecular Biopharmacy and Genetics, Graduate School of Pharmaceutical Sciences, and the [4]New Industry Creation Hatchery Center, Tohoku University, Sendai, Japan.

Supported in part by a Grant-in-Aid for Scientific Research from Japan Society for the Promotion of Science, the Nakatomi Foundation, the Suzuken Memorial Foundation, and the Mochida Memorial Foundation for Medical and Pharmaceutical Research.

Submitted for publication May 22, 2003; revised August 9 and December 25, 2003; accepted January 5, 2004.

Disclosure: **K.-I. Hosoya**, None; **A. Minamizono**, None; **K. Katayama**, None; **T. Terasaki**, None; **M. Tomi**, None

The publication costs of this article were defrayed in part by page charge payment. This article must therefore be marked "*advertisement*" in accordance with 18 U.S.C. §1734 solely to indicate this fact.

Corresponding author: Ken-ichi Hosoya, Faculty of Pharmaceutical Sciences, Toyama Medical and Pharmaceutical University, 2630, Sugitani, Toyama 930-0194, Japan; hosoyak@ms.toyama-mpu.ac.jp.

Investigative Ophthalmology & Visual Science, April 2004, Vol. 45, No. 4

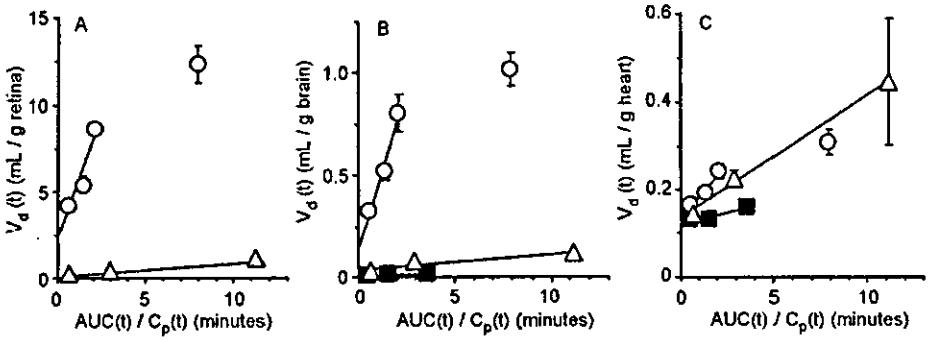

FIGURE 1. Integration plot of the initial uptake of [^{14}C]DHA, [^{14}C]AA, and [^{3}H]D-mannitol by the retina (A), brain (B), and heart (C) after intravenous administration. [^{14}C]DHA (○, 5 μCi/rat), [^{14}C]AA (△, 10 μCi/rat), or [^{3}H]D-mannitol (■, 10 μCi/rat) was injected into the femoral vein. The counts of [^{3}H]D-mannitol uptake by the retina were close to background. Each point represents the mean ± SEM (n = 3–5).

MATERIALS AND METHODS

Animals

Male Wistar rats, weighing 250 to 300 g, were purchased from SLC (Shizuoka, Japan). The investigations using rats described in this report conformed to the provisions of the Animal Care Committee, Toyama Medical and Pharmaceutical University (2001-190) and the ARVO Statement for the Use of Animals in Ophthalmic and Vision Research.

Reagents

L-[1-^{14}C]Ascorbic acid ([^{14}C]AA, 13 mCi/mmol) and D-[1-^{3}H(N)]mannitol ([^{3}H]D-mannitol, 17 Ci/mmol) were purchased from PerkinElmer Life Sciences (Boston, MA). L-[^{14}C]Dehydroascorbic acid ([^{14}C]DHA, purity more than 90%; see Fig. 2B) was generated in all experiments by incubating [^{14}C]AA (1 μM in saline) with ascorbate oxidase (1 unit/1 mmol AA in saline; Sigma-Aldrich, St. Louis, MO) at 37°C for 90 seconds, according to a reported method.[16] All other chemicals were of reagent grade and available commercially.

Blood-to-Retina Transport Studies

A Wistar rat was anesthetized with an intramuscular injection of ketamine-xylazine (1.22 mg/kg xylazine and 125 mg/kg ketamine). The femoral artery was cannulated with polyethylene tubing (SP-31, inner diameter 0.5 mm, outer diameter 0.8 mm; Natsume, Tokyo, Japan) containing 100 IU heparin/mL in extracellular fluid buffer (122 mM NaCl, 25 mM $NaHCO_3$, 3 mM KCl, 1.4 mM $CaCl_2$, 1.2 mM $MgSO_4$, 0.4 mM K_2HPO_4, 10 mM D-glucose, and 10 mM HEPES [pH 7.4]) to collect blood samples. Then, [^{14}C]DHA (5 μCi/rat), [^{14}C]AA (10 μCi/rat), or [^{3}H]D-mannitol (10 μCi/rat) was injected into the femoral vein. After collection of blood samples, all rats were decapitated, and the retinas, cerebrum, and heart were removed. All samples were dissolved in 2 N NaOH at 50°C for 3 hours. After the samples were dissolved, 50 μL H_2O_2 was added to the blood and heart samples to decolorize them. All samples were neutralized and mixed with liquid scintillation cocktail (ACS II; Amersham, Buckinghamshire, UK) and then the radioactivity was measured in a liquid scintillation counter (LS6500; Beckman-Coulter, Fullerton, CA).

Determination of Influx Permeability Clearance

The apparent influx permeability clearance (K_{in}) of [^{14}C]DHA, [^{14}C]AA, or [^{3}H]D-mannitol in tissues was determined by integration plot analysis,[19,20] by modification of a reported method.[20] Briefly, the tissue uptake of each compound can be expressed as

$$dX(t)/dt = K_{in} \times C_p(t) - K_{eff} \times X(t) \quad (1)$$

where $X(t)$ (dpm/g tissue) and $C_p(t)$ (dpm/mL) are the tissue concentration and plasma concentration at time t, respectively, and K_{in} and K_{eff} represent the influx and efflux permeability clearance in tissue, respectively. Integrating equation 1 and solving the apparent tissue concentration in the early-phase gives

$$X_{app}(t) = K_{in} \times AUC(t) + V_i \times C_p(t) \quad (2)$$

where $X_{app}(t)$ (dpm/g tissue) is the apparent tissue concentration in the sample, AUC(t) (dpm · min/mL) is the area under the plasma concentration time curve of each compound from time 0 to t and V_i (mL/g tissue) is the volume of interstitial space in the tissue. Division of both sides of equation 2 by $C_p(t)$ gives

$$X_{app}(t)/C_p(t) = K_{in} \times AUC(t)/C_p(t) + V_i \quad (3)$$

The apparent tissue-to-plasma concentration ratio [$V_d(t)$] (mL/g tissue) is defined as $X_{app}(t)/C_p(t)$

$$V_d(t) = K_{in} \times AUC(t)/C_p(t) + V_i \quad (4)$$

when AUC(t)/C_p(t) (minute) is plotted versus $V_d(t)$, as shown in Figure 1, the early-phase slope represents the K_{in} in the tissue (μL/(min · g tissue)). The apparent influx permeability clearances of [^{14}C]DHA, [^{14}C]AA, or [^{3}H]D-mannitol in retina ($K_{in,\ retina}$), brain ($K_{in,\ brain}$), and heart ($K_{in,\ heart}$) were determined.

High-Performance Liquid Chromatography Analysis

The purity of [^{14}C]DHA prepared in each experiment, and the metabolism of [^{14}C]DHA in plasma and retina were determined by high-performance liquid chromatography (HPLC). Thirty seconds or 5 minutes after intravenous injection, plasma and retinas were collected and frozen with dry ice. The frozen sample of retina was homogenized in 70% MeOH, and plasma was mixed with 70% MeOH. After centrifugation at 12,550g for 5 minutes, an aliquot of the samples was subjected to HPLC, using a system equipped with an anion exchange column (TSK-Gel NH_2-60; Tosoh, Tokyo, Japan). The mobile phase consisted of 35% 0.05 M KH_2PO_4-65% CH_3CN at a flow rate of 1.0 mL/min. The eluent was collected in vials, and the radioactivity in each fraction was determined by liquid scintillation counting.

[^{14}C]DHA and [^{14}C]AA Uptake by TR-iBRB2 Cells

The conditionally immortalized rat retinal capillary endothelial cell line (TR-iBRB2), which had been established and characterized,[21–23] was used as an in vitro inner BRB model to characterize DHA and AA transport. TR-iBRB2 cells express GLUT1 protein and have functional 3-O-methyl-D-glucose (3-OMG) transport, with a K_m of 5.56 mM.[21] TR-iBRB2 cells (passages 27–38) were cultured at 33°C in Dulbecco's modified Eagle's medium (Nissui Pharmaceutical Co., Tokyo, Japan) in 5% CO_2-air, as described previously.[21] For the uptake study, cells (5×10^4 cells/cm^2) were cultured at 33°C for 2 days on a rat tail collagen-type I–coated 24-well plate (BD Biosciences, San Jose, CA) and washed with 1 mL uptake buffer (134 mM NaCl, 5.2 mM KCl, 0.8 mM $MgSO_4$, 1.8 mM $CaCl_2$, and 20 mM HEPES [pH 7.5]) at 37°C. Uptake was initiated by applying 200 μL uptake buffer containing 0.2 μCi [^{14}C]DHA (69.2 μM) or [^{14}C]AA (76.9 μM) at 37°C in the presence or

absence of inhibitors. For the concentration-dependent study, a concentration range of DHA from 1.7 to 180 μM was prepared using [^{14}C]DHA from 4.9 nCi to 4.4 μCi. Na^+-free uptake buffers were prepared in two different ways. The choline- and Li^+-buffers were prepared by equimolar replacement of NaCl with choline chloride and LiCl, respectively. After a predetermined time period, uptake was terminated by removing the solution, and cells were immersed in ice-cold uptake buffer and solubilized. [^{14}C]DHA in the uptake buffer was stable over the uptake study period of 3 minutes. Radioactivity was measured by liquid scintillation counting, and the protein content was determined with a kit (DC; Bio-Rad, Hercules, CA) with bovine serum albumin (BSA) as a standard.

RT-PCR Analysis

Total cellular RNA was prepared from phosphate-buffered saline (PBS)-washed cells using a kit (RNeasy Mini Kit; Qiagen, Hilden, Germany). Single-strand cDNA was made from 1 μg total RNA by reverse transcription (RT), using oligo dT primer. The polymerase chain reaction (PCR) was performed with a gene amplification system (GeneAmp PCR system 9700; Applied Biosystems, Foster City, CA) with GLUT1-, GLUT3-, SVCT1-, SVCT2-, and β-actin-specific primers through 25 cycles of 94°C for 30 seconds, 60°C for 1 minute, and 72°C for 1 minute. The sequences of the specific primers were as follows: sense, 5′-GAT GAT GAA CCT GTT GGC CT-3′; antisense, 5′-AGC GGA CAG CTC CAA GAT G-3′ for rat GLUT1 (Slc2a1, GenBank accession number NM_138827; http://www.ncbi.nlm.nih.gov/Genbank; provided in the public domain by the National Center for Biotechnology Information, Bethesda, MD); sense, 5′-GAC GAG AGT ATC AGG ATG TCA CAG-3′; antisense, 5′-AGG CCA CGT AGA CCA AGA TAG CC-3′ for rat GLUT3 (Slc2a3, GenBank accession number NM_017102); sense, 5′-CCT GTT TAC CGA TGG GGC AAG G-3′ antisense, 5′-ACT CGA TGA TGC CCG CCA GTG T-3′ for rat SVCT1 (Slc23a2, GenBank accession number NM_017316); sense, 5′-ACA CCA CAG AGA TCA CAG TTG CC-3′; antisense, 5′-TGT AAC TTG TAG GCC GTC CAT CC-3′ for rat SVCT2 (Slc23a1, GenBank accession number NM_017315); sense, 5′-TCA TGA AGT GTG ACG TTG ACA TCC GT-3′, antisense, 5′-CCT AGA AGC ATT TGC GGT GCA CGA TG-3′ for the β-actin (GenBank accession number NM_031144). The PCR products were separated by electrophoresis on an agarose gel in the presence of ethidium bromide and visualized under ultraviolet light. The molecular identity of the resultant product was confirmed by restriction analysis with two different restriction enzymes or sequence analysis using a DNA sequencer (Prism 310; Applied Biosystems).

Quantitative Real-Time PCR

Quantitative real-time PCR was performed on a sequence detection system (Prism 7700 with 2× SYBR Green PCR Master Mix; Applied Biosystems) according to the manufacturer's protocol. To quantify the amount of specific mRNA in the samples, a standard curve was generated for each run using a plasmid (pGEM-T Easy Vector; Promega, Madison, WI) containing the gene of interest. This enabled standardization of the initial mRNA content of cells relative to the amount of β-actin. The PCR was performed using rat GLUT1-, GLUT3-, SVCT2-, or β-actin-specific primers, and the cycling parameters were those given for RT-PCR analysis.

Immunostaining Analysis

Cells were cultured on a rat tail collagen-type I–coated coverslip (BD Biosciences, Lincoln Park, NJ) at 33°C for 48 hours. After removal of medium, cells were washed with PBS and fixed in 4% formaldehyde-PBS for 10 minutes at room temperature. Cells were permeated with 0.2% Triton X-100 in PBS for 15 minutes and incubated with blocking agent solution (Block Ace; Dainihon Pharmaceutical Co., Osaka, Japan) for 60 minutes. After washing with PBS, cells were further incubated with rabbit anti-GLUT1 antibody (Chemicon, Temecula, CA), rabbit anti-GLUT3 antibody (Chemicon) or goat anti-SVCT2 antibody (1:200 dilution; Santa Cruz Biotechnology, Santa Cruz, CA) as a primary antibody with 1% BSA for 3 hours at room temperature. Cells were washed with PBS and incubated for 1 hour at room temperature with FITC-conjugated anti-rabbit IgG (Chemicon) or FITC-conjugated anti-goat IgG (Chemicon) (1:50 dilution) as a secondary antibody. Cells were subsequently stained with propidium iodide and viewed by confocal laser scanning microscope (LSM 510; Carl Zeiss Meditec, Oberkochen, Germany). The control experiments were performed in parallel, with normal rabbit or goat IgG used instead of the primary antibody.

Data Analysis

The uptake of [^{14}C]DHA and [^{14}C]AA by TR-iBRB2 cells was expressed as the cell-to-medium (cell/medium) ratio

$$\text{Cell/medium ratio} = ([^{14}\text{C}]\ \text{dpm per mg cell protein})/([^{14}\text{C}]\ \text{dpm per } \mu\text{L medium}) \quad (5)$$

The [^{3}H]D-mannitol uptake study was performed to estimate the volume of adhering water. The resultant cell/medium ratio was 0.1 to 0.2 μL/mg protein, more than 10 times lower than that of [^{14}C]DHA. Therefore, adhering water was ignored when calculating the cell/medium ratio.

For kinetic studies, the K_m and the maximum uptake rate (J_{max}) of DHA were calculated, using the nonlinear least-squares regression analysis program, MULTI[24]

$$J = J_{max} \times [S]/(K_m + [S]) \quad (6)$$

where J and $[S]$ are the uptake rate of DHA at 1 minute and the concentration of DHA, respectively.

The 50% inhibition concentration (IC_{50}) of D-glucose for [^{14}C]DHA uptake by TR-iBRB2 cells was calculated by fitting the data to a sigmoidal inhibition model[25] using MULTI[24]

$$V = V_0/[1 + ([I]/IC_{50})^n] \quad (7)$$

where V and V_0 are the uptake of [^{14}C]DHA in the presence and absence of D-glucose, respectively, and $[I]$ and n is the concentration of D-glucose and the Hill coefficient, respectively.

Unless otherwise indicated, all data are expressed as the mean ± SEM. Statistical significance of differences among means of several groups was determined by one-way analysis of variance (ANOVA) followed by the modified Fisher least-squares difference method.

Results

Blood-to-Retina Transport of Vitamin C across the BRB

The in vivo blood-to-retina influx transport of DHA, AA, and D-mannitol across the BRB was evaluated and compared with other tissues by means of the integration plot analysis after intravenous administration of each of the radio-labeled compounds to rats (Fig. 1). The $K_{in,\ retina}$ of [^{14}C]DHA was determined to be 2.44×10^3 μL/(min · g retina) from the slope representing the apparent influx permeability clearance across the BRB, using equation 4, whereas the $K_{in,\ retina}$ of [^{14}C]AA was 65.4 μL/(min · g retina) (Fig. 1A; Table 1). $K_{in,\ retina}$ for [^{14}C]DHA was 37.3-fold greater than that for [^{14}C]AA. A similar difference was observed in the brain: 38.1 for the ratio between the $K_{in,\ brain}$ of [^{14}C]DHA and [^{14}C]AA, whereas it was only 3.79 in the heart, which does not have a barrier between blood and organ (Figs. 1B, 1C; Table 1). In the comparison between retina and brain, the $K_{in,\ retina}$ of [^{14}C]DHA and [^{14}C]AA was approximately eight times greater than the $K_{in,\ brain}$, indicating that vitamin C transport across the BRB is greater

TABLE 1. The Apparent Influx Permeability Clearance (K_{in}) per Gram Rat Tissue and Blood/Plasma Ratio (R_B) of [^{14}C]DHA, [^{14}C]AA, and [^{3}H]D-Mannitol

Groups	$K_{in,\ retina}$ (μl/(min · g retina))	$K_{in,\ brain}$ (μl/(min · g brain))	$K_{in,\ heart}$ (μl/(min · g heart))	R_B
[^{14}C]DHA	$2.44\times10^{3} \pm 0.05\times10^{3}$	309 ± 53	49.7 ± 15.1	0.65 ± 0.01
[^{14}C]AA	65.4 ± 10.5	8.12 ± 1.34	13.1 ± 11.0	ND
[^{3}H]D-Mannitol	ND	1.65 ± 0.38	10.8 ± 5.25	0.58 ± 0.03

K_{in} was estimated from the initial slope in Figure 1 and is expressed as the mean ± SD. R_B was determined at 3 minutes after intravenous administration of [^{14}C]DHA or [^{3}H]D-mannitol and is expressed as the mean ± SEM (n = 3). ND, not determined.

than that across the BBB. To examine whether blood cells in capillaries contribute to concentrative uptake in the retina, the apparent concentration ratio between blood and plasma (R_B) was measured. The R_B of [^{14}C]DHA were constant over 10 minutes and not much different from that of [^{3}H]D-mannitol at 3 minutes after administration (Table 1). These results support the hypothesis that the blood-to-retina DHA transport is much greater than that of AA.

Figure 2 shows the HPLC chromatograms of [^{14}C]DHA and [^{14}C]AA present in the retina and plasma after intravenous administration of 5 μCi [^{14}C]DHA. [^{14}C]DHA in plasma was rapidly changed into AA after administration and almost all the [^{14}C]DHA was converted in 5 minutes (Figs. 2E, 2F). [^{14}C]DHA accumulated in the retina as AA in a time-dependent manner (Figs. 2C, 2D).

[^{14}C]DHA and [^{14}C]AA Uptake by TR-iBRB2 Cells

To elucidate the transport mechanism of DHA, TR-iBRB2 cells were used as an in vitro rat inner BRB model.[21-23] The [^{14}C]DHA and [^{14}C]AA uptakes by TR-iBRB2 cells exhibited time-dependent increases for at least 3 minutes, with an initial uptake rate of 25.6 μL/(min · mg protein) and 0.700 μL/(min · mg protein), respectively (Fig. 3A). The uptake clearance of [^{14}C]DHA in TR-iBRB2 cells was 36.6 times greater than that of [^{14}C]AA. The [^{14}C]DHA uptake by TR-iBRB2 cells under Na^+-free conditions, using choline- or Li^+-uptake buffer, was not significantly different from the control (Na^+-uptake buffer; Fig. 3B). The [^{14}C]DHA uptake by TR-iBRB2 cells took place in a concentration-dependent manner with a K_m of 93.4 ± 18.8 μM and a J_{max} of 10.7 ± 1.2 nmol/(min · mg protein) (mean ± SD; Fig. 4), indicating that DHA is transported through an Na^+-independent carrier-mediated transport system in TR-iBRB2 cells.

Inhibitory Effect of Several Compounds on [^{14}C]DHA Uptake

The effect of glucose transporters' substrates and inhibitors on [^{14}C]DHA uptake by TR-iBRB2 cells is summarized in Table 2. D-Glucose, 3-OMG, and 2-deoxyglucose (2-DG), glucose transporters' substrates, at 30 mM, caused marked inhibition (86.4%, 81.1%, and 90.9%, respectively). L-Glucose at 30 mM caused no significant inhibition. Phloretin and cytochalasin B, glucose transporter inhibitors, at 10 μM, produced an inhibition of 60.8% and 83.4%, respectively, whereas the same concentration of phlorizin and cytochalasin E as a control for phloretin and cytochalasin B, respectively, did not have any significant effect. This inhibition of [^{14}C]DHA uptake supports the hypothesis that facilitative glucose transporters are involved in the uptake process by TR-iBRB2 cells. Moreover, [^{14}C]DHA uptake was inhibited by D-glucose in a concentration-dependent manner with an IC_{50} of 5.56 ± 0.57 mM (mean ± SD; Fig. 5).

Expression of GLUT1, GLUT3, SVCT1, and SVCT2 in TR-iBRB2 Cells

To determine vitamin C transporter expression in TR-iBRB2 cells, we performed RT-PCR analysis, using total RNA isolated

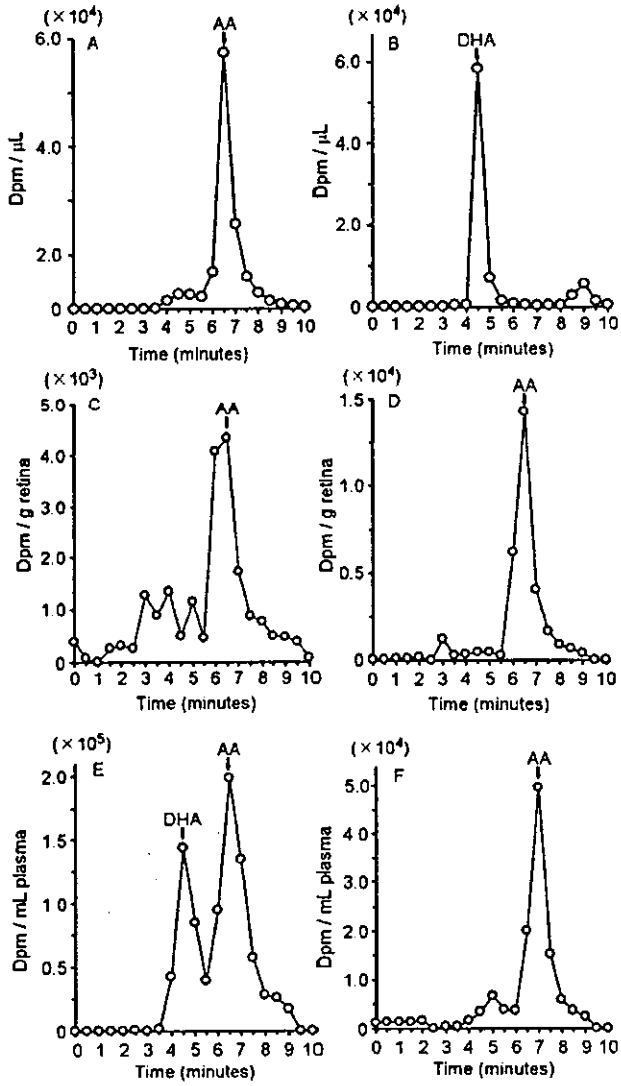

FIGURE 2. Typical HPLC chromatogram of samples of retina (C, D) and plasma (E, F) after intravenous administration of [^{14}C]DHA (B). [^{14}C]DHA was generated by incubating [^{14}C]AA (A) with ascorbate oxidase (1 U/1 mmol AA). [^{14}C]DHA (5 μCi/rat) was injected into the femoral vein, and retinas and plasma were collected at 30 seconds (C, E) and 5 minutes (D, F).

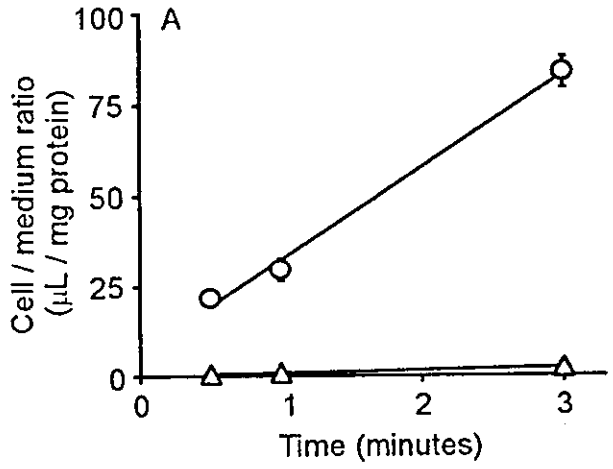

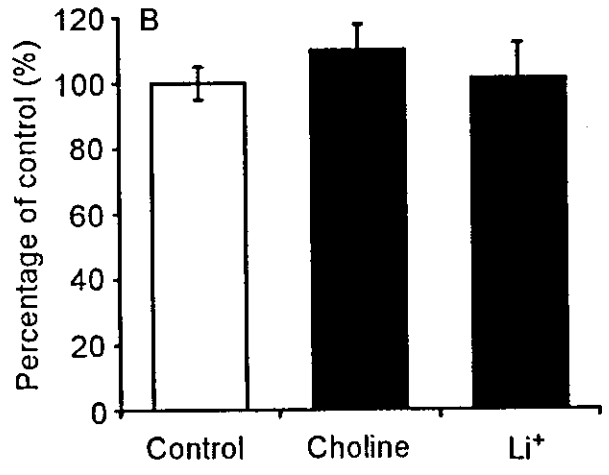

FIGURE 3. Time-course of [^{14}C]DHA and [^{14}C]AA uptake (A) and Na^+ independence of [^{14}C]DHA uptake by TR-iBRB2 cells (B). (A) [^{14}C]DHA (○, 0.2 μCi) and [^{14}C]AA (△, 0.2 μCi) uptake were performed at 37°C. (B) [^{14}C]DHA (0.2 μCi) uptake was performed in the presence or absence of Na^+ (Na^+ was replaced with equimolar choline or Li^+) at 1 minute and at 37°C. The uptake was expressed as the cell/medium ratio according to equation 5. Each point represents the mean ± SEM (n = 4).

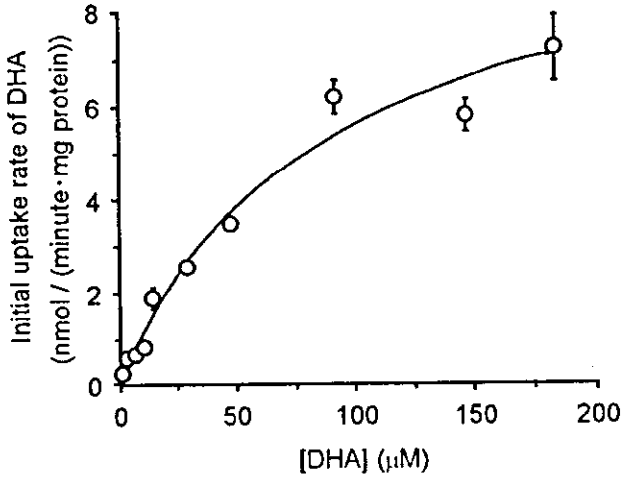

FIGURE 4. Concentration-dependence of DHA uptake by TR-iBRB2 cells. [^{14}C]DHA uptake was performed at 2 minutes at 37°C, over the concentration range from 1.7 μM (4.9 nCi) to 180 μM (4.4 μCi). Data are the mean ± SEM (n = 4). The K_m and J_{max} were 93.4 ± 18.8 μM and 10.7 ± 1.2 nmol/(min · mg protein), respectively (mean ± SD).

from TR-iBRB2 cells, brain, and kidney and specific primers of rat GLUT1 and -3 and rat SVCT1 and -2 (Fig. 6A). β-Actin was used as a housekeeping gene. GLUT1, GLUT3, and SVCT2 mRNA were amplified at 503, 398, and 358 bp, respectively, in TR-iBRB2 cells and brain, whereas SVCT1 mRNA was not. The mRNA expression levels of GLUT1, GLUT3, and SVCT2 were determined in TR-iBRB2 cells by quantitative real-time PCR analysis. The quantity of expression mRNA, compensated with β-actin, for GLUT1, GLUT3, and SVCT2 was $7.39 \times 10^{-3} \pm 0.91 \times 10^{-3}$, $1.98 \times 10^{-4} \pm 0.25 \times 10^{-4}$, and $1.84 \times 10^{-5} \pm 0.26 \times 10^{-5}$, respectively (Fig. 6B). Accordingly, the expression of GLUT1 mRNA was 37.3 and 402 times greater, respectively, than that of GLUT3 and SVCT2 mRNA in TR-iBRB2 cells.

The expression and localization of GLUT1, GLUT3, and SVCT2 protein in TR-iBRB2 cells were examined by confocal laser scanning microscope (Fig. 7). The immunostaining by anti-GLUT1 (Figs. 7A, 7D) and anti-GLUT3 antibody (Figs. 7B, 7E) was observed in TR-iBRB2 cells. No significant fluorescence was observed in TR-iBRB2 cells stained with anti-SVCT2 antibody (Figs. 7C, 7F) and normal IgG (data not shown). An x-z section in GLUT1 and GLUT3 staining (Figs. 7D, 7E) showed that fluorescence (green) was located over the cell nucleus (red), providing supporting evidence that GLUT1 and GLUT3 are mainly localized on the cell surface of TR-iBRB2 cells.

DISCUSSION

The present study produces, for the first time, in vivo evidence that vitamin C is mainly transported as DHA across the BRB and accumulates as AA in the retina (Figs. 1 and 2). DHA is transported by a facilitative glucose transporter, most likely GLUT1, which is expressed at the luminal (blood) and abluminal (retina) side of the inner BRB and RPE (outer BRB),[17] although the additional contribution of GLUT3 cannot be ruled out at the present time.[26] GLUT1 mRNA expression in TR-iBRB2 cells used as an in vitro model of inner BRB was 37 times greater than that of GLUT3. Nevertheless, GLUT1 and -3 proteins were substantially expressed on the cell surface of TR-iBRB2 cells (Figs. 6, 7). [^{14}C]DHA uptake by TR-iBRB2 cells took place in an Na^+-independent and concentration-dependent manner, with a K_m of 93.4 μM (Figs. 3B, 4). This K_m is similar to that

TABLE 2. Inhibitory Effect of Several Compounds on [^{14}C]DHA Uptake by TR-iBRB2 Cells

Inhibitors	Percentage of Control
Control	100 ± 12
30 mM D-Glucose	13.6 ± 3.1*
30 mM L-Glucose	81.3 ± 2.7
30 mM 3-OMG	18.9 ± 1.3*
30 mM 2-DG	9.10 ± 1.8*
10 μM Phloretin	39.2 ± 8.3*
10 μM Phloridzin	91.7 ± 8.9
10 μM Cytochalasin B	16.6 ± 7.5*
10 μM Cytochalasin E	100.3 ± 4.6

[^{14}C]DHA uptake was performed for 2 minutes at 37°C in the presence or absence of inhibitors. Data are expressed as the mean ± SEM (n = 4–12). 3-OMG: 3-O-methyl-D-glucose, 2-DG: 2-deoxyglucose.
* $P < 0.01$, significantly different from control.

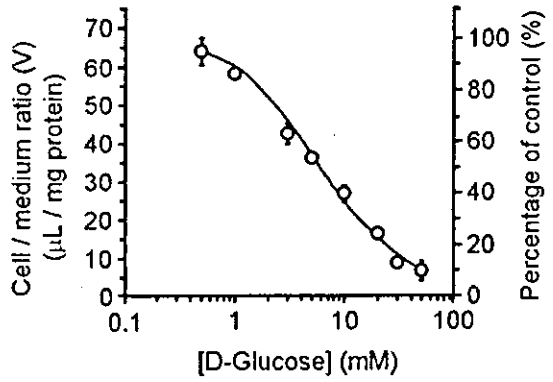

FIGURE 5. Inhibitory effect of D-glucose on [^{14}C]DHA uptake by TR-iBRB2 cells. [^{14}C]DHA uptake was performed in the presence (0.5–50 mM) or absence (control) of D-glucose at 2 minutes and at 37°C. Each point represents the mean ± SEM (n = 4). The IC_{50} is 5.56 ± 0.57 mM (mean ± SD).

obtained for DHA uptake (K_m = 60 μM) in *Xenopus* oocytes expressing GLUT1.[12] Moreover, [^{14}C]DHA uptake by TR-iBRB2 cells was strongly inhibited by glucose transporter substrates, such as D-glucose, 3-OMG, and 2-DG and inhibitors, such as phloretin and cytochalasin B (Table 2).[27]

The $K_{in,\ retina}$ of [^{14}C]DHA (2.44 × 10^3 μL/(min · g retina)) was 37 times greater than that of [^{14}C]AA (65.4 μL/(min · g retina); Fig. 1A). This result agrees with the ratio between [^{14}C]DHA and [^{14}C]AA uptake clearance in TR-iBRB2 cells (Fig. 3A) and supports the hypothesis that DHA is predominantly transported through facilitative glucose transporters at the BRB rather than by AA. However, AA transport into the retina cannot be fully ruled out at the present time, because the $K_{in,\ retina}$ of [^{14}C]AA was significantly greater than that of [^{3}H]D-mannitol, which was used as a nonpermeable paracellular marker (Fig. 1A). In addition, an Na^+-dependent AA transport process seems to be present in the bovine RPE.[10] In the brain, a similar difference in the $K_{in,\ brain}$ between [^{14}C]DHA and [^{14}C]AA supports the hypothesis that glucose transporters at the blood–organ barriers such as the BRB and BBB facilitate transport of DHA, but not of AA, as reported at the BBB,[16] since, in the heart, there was not a great difference in the $K_{in,\ heart}$ between [^{14}C]DHA and [^{14}C]AA (Table 1). The $K_{in,\ retina}$ of [^{14}C]DHA and [^{14}C]AA was approximately eight times greater than the corresponding values in brain (Table 1). Possible reasons for this are that the amounts of retinal and brain capillary endothelial cells represent a small percentage of the weight of the entire retina and 0.1% to 0.2% of the weight of the entire brain, respectively,[28,29] and RPE (outer BRB) contributes to the supply of essential molecules in the outer segment of the retina, whereas choroid plexus epithelial cells (blood–cerebrospinal fluid barrier) do not play a major role in supplying them for the entire brain.[7,30] Moreover, Root-Bernstein et al.[31] reported the evidence that DHA, rather than AA, is taken up by human RPE, and its uptake is inhibited by D-glucose in a concentration-dependent manner.[31] GLUT1 expression in rat retinal capillary endothelial cells is greater than that in rat brain capillary endothelial cells.[32,33]

The innate vitamin C regulatory mechanism in the retina most likely involves GLUT1 supplying DHA to the retina at the luminal and abluminal sides of the inner BRB and RPE (outer BRB), and the transported DHA is reduced to AA and accumulates in the retina as an antioxidant. Even though GLUT1 is not a concentrative transporter, DHA is rapidly reduced to AA and thus is trapped within the retina (Fig. 2). The conversion of [^{14}C]DHA to [^{14}C]AA in plasma is very rapid compared with the initial uptake of [^{14}C]DHA (Figs. 1, 2). The level of [^{14}C]DHA remaining in plasma seems to be underestimated, because it cannot be ignored that [^{14}C]DHA converts to [^{14}C]AA during manipulation of the assay.[34] Notably, blood-to-retina influx transport of [^{14}C]DHA takes place, since it was much greater than that of [^{14}C]AA (Fig. 1, Table 1). Although the affinity of DHA for facilitative glucose transporters (K_m = 93.4 μM, Fig. 4) is greater than that of D-glucose, (the K_m estimated for D-glucose uptake by the retina across the rat BRB was 7.81 mM),[35] DHA uptake through facilitative glucose transporters is competitively inhibited by D-glucose, and the normal plasma D-glucose concentration in most mammals is approximately 5 mM. D-Glucose inhibited [^{14}C]DHA uptake by TR-

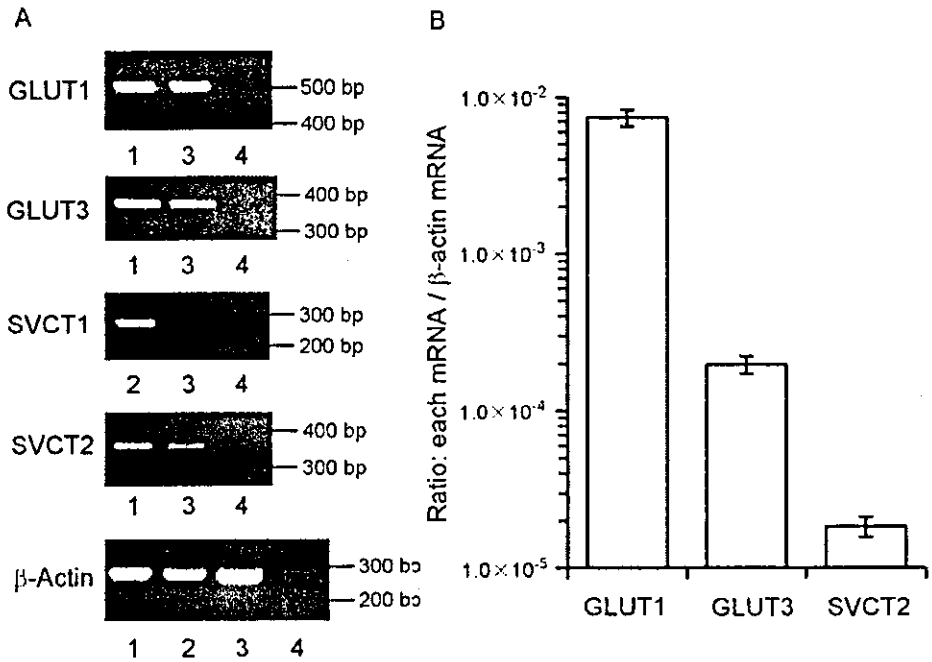

FIGURE 6. RT-PCR analysis of GLUT1, GLUT3, SVCT1, SVCT2, and β-actin (A) and the amount of GLUT1, GLUT3, and SVCT2 mRNA (B) in TR-iBRB2 cells. (A) *lane 1*: rat brain; *lane 2*: rat kidney; *lane 3*: TR-iBRB2 cells; *lane 4*: in the absence of reverse transcriptase for TR-iBRB2 cells. Rat brain was used as a positive control for GLUT1, GLUT3, and SVCT2, and rat kidney was used as a positive control for SVCT1. (B) The amount of GLUT1, GLUT3, and SVCT2 mRNA in TR-iBRB2 cells was determined by quantitative real-time PCR analysis. Data are the mean ± SEM (n = 4). The GLUT1, GLUT3, and SVCT2 mRNA content relative to β-actin mRNA (GLUT1/β-actin, GLUT3/β-actin, and SVCT2/β-actin) was 7.39 × 10^{-4} ± 0.91 × 10^{-4}, 1.98 × 10^{-4} ± 0.25 × 10^{-4}, and 1.84 × 10^{-5} ± 0.26 × 10^{-5}, respectively.

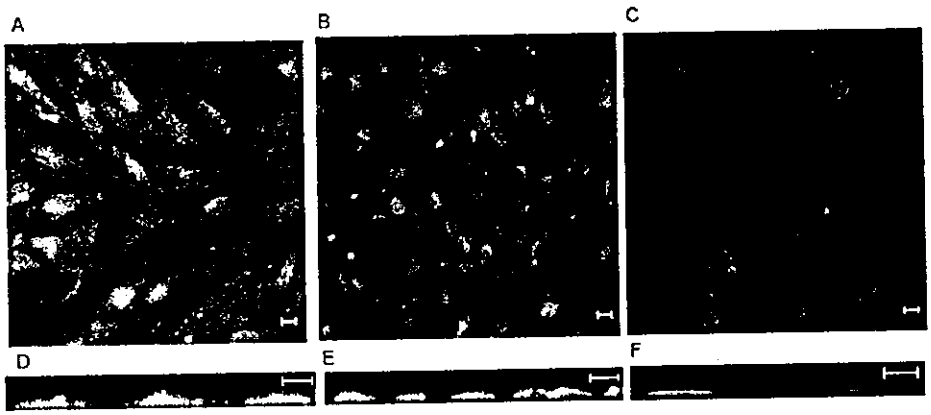

FIGURE 7. Immunostaining analysis of GLUT1, GLUT3, and SVCT2 in TR-iBRB2 cells. TR-iBRB2 cells were immunostained by anti-GLUT1 (A, D), anti-GLUT3 (B, E), and anti-SVCT2 (C, F) antibodies. (A, B, C) *x-y* sections; (D, E, F) *x-z* sections. *Green*: immunoreactivity by each antibody; *red*: nuclei stained by propidium iodide. Scale bar, 10 μm.

iBRB2 cells, with an IC_{50} of 5.56 mM (Fig. 5). Therefore, DHA transport by facilitative glucose transporters across the BRB does not exhibit complete inhibition (i.e., approximately 50%), under normal conditions. The DHA plasma concentration has been recently determined to be approximately 10 μM (10%–20% of total plasma ascorbate concentration) in the rat and human.[14,15] Moreover, DHA is produced by metal-binding proteins, such as serum albumin and by superoxide anions in endothelial cells.[36,37] However, hyperglycemia (i.e., diabetic mellitus) increases the blood D-glucose concentration to 20 mM or higher, leading to the inhibition of DHA transport at the BRB.[31] Indeed, [^{14}C]DHA uptake by TR-iBRB2 cells was inhibited by 79% at a concentration of 20 mM D-glucose (Fig. 5). Although there is contradictory evidence showing regulation of GLUT1 expression in retinal capillary endothelial cells under diabetic conditions,[33,38] rats with streptozotocin-induced diabetes show downregulation of GLUT1 expression by 50% in the retina.[33] In light of these findings, diabetic patients may experience enhanced oxidative stress in the retina because of reduced influx of DHA, leading to the hypothesis that diabetic retinopathy involves dysfunction of DHA influx at the BRB.

From a pharmacological viewpoint, intravenous administration of DHA may be effective for retinal ischemia-reperfusion to protect the neural retina against oxidative stress. Huang et al.[39] reported that intravenous administration of DHA mediates cerebroprotection after reperfused and nonreperfused cerebral ischemia, but this did not happen with AA. This suggests that DHA can use a transportable prodrug of AA across the BRB and BBB to exert its neuroprotective effects. However, DHA has membrane-disruptive effects in erythrocytes and renal brush border membrane and may destroy the pancreatic beta cells.[40,41] Further studies are needed to elucidate the relationship between pharmacologically effective and toxicologically adverse concentrations of DHA in plasma.

In conclusion, vitamin C is predominantly transported as DHA through facilitative glucose transporters at the BRB and accumulates as AA in the retina. The physiological role of facilitative glucose transporters at the BRB appears to involve the supply of vitamin C from the circulating blood to the retina to protect the neural retina against oxidative stress. These findings provide important information to help us understand the physiological and pathophysiological roles of facilitative glucose transporters at the BRB and assist in the design of a suitable DHA dosage regimen for pharmacological therapies.

Acknowledgments

The authors thank Hisashi Iizasa and Masanori Tachikawa for valuable discussion.

References

1. Friedman PA, Zeidel ML. Victory at C. *Nat Med*. 1999;5:620–621.
2. Ham WT Jr, Mueller HA, Ruffolo JJ Jr, et al. Basic mechanisms underlying the production of photochemical lesions in the mammalian retina. *Curr Eye Res*. 1984;3:165–174.
3. Woodford BJ, Tso MOM, Lam KW. Reduced and oxidized ascorbates in guinea pig retina under normal and light-exposed conditions. *Invest Ophthalmol Vis Sci*. 1983;24:862–867.
4. Nielsen JC, Naash MI, Anderson RE. The regional distribution of vitamin E and C in mature and premature human retinas. *Invest Ophthalmol Vis Sci*. 1988;29:22–26.
5. Greco AM, Fioretti F, Rino A. Relationship between hemorrhagic ocular disease and vitamin C deficiency: clinical and experimental data. *Acta Vitaminol Enzymol*. 1980;2:21–25.
6. Kowluru RA, Tang J, Kern TS. Abnormalities of retinal metabolism in diabetes and experimental galactosemia. *Diabetes*. 2001;50:1938–1942.
7. Cunha-Vaz JG. The blood-retinal barriers. *Doc Ophthalmol*. 1976;41:287–327.
8. Stewart PA, Tuor UI. Blood-eye barriers in the rat: correlation of ultrastructure with function. *J Comp Neurol*. 1994;340:566–576.
9. Tsukagoshi H, Tokui T, Mackenzie B, et al. A family of mammalian Na^+-dependent L-ascorbic acid transporters. *Nature*. 1999;399:70–75.
10. Khatami M. Na^+-linked active transport of ascorbate into cultured bovine retinal pigment epithelial cells: heterologous inhibition by glucose. *Membr Biochem*. 1987–1988;7:115–130.
11. Kannan R, Stolz A, Ji Q, Prasad PD, Ganapathy V. Vitamin C transport in human lens epithelial cells: evidence for the presence of SVCT2. *Exp Eye Res*. 2001;73:159–165.
12. Vera JC, Rivas CI, Fischbarg J, Golde DW. Mammalian facilitative hexose transporters mediate the transport of dehydroascorbic acid. *Nature*. 1993;364:79–82.
13. Rumsey SC, Kwon O, Xu GW, Burant CF, Simpson I, Levine M. Glucose transporter isoforms GLUT1 and GLUT3 transport dehydroascorbic acid. *J Biol Chem*. 1997;272:18982–18989.
14. Koshiishi I, Imanari T. Quantification of carbamylated dehydroascorbate derivative produced from cyanate and dehydroascorbate. *J Chromatogr B*. 1998;709:150–156.
15. Nakayama H, Akiyama S, Inagaki M, Gotoh Y, Oguchi K. Dehydroascorbic acid and oxidative stress in haemodialysis patients. *Nephrol Dial Transplant*. 2001;16:574–579.
16. Agus DB, Gambhir SS, Pardridge WM, et al. Vitamin C cross the blood-brain barrier in the oxidized form through the glucose transporters. *J Clin Invest*. 1997;100:2842–2848.
17. Takata K, Kasahara T, Kasahara M, Ezaki O, Hirano H. Ultracytochemical localization of the erythrocyte/HepG2-type glucose transporter (GLUT1) in cells of the blood-retinal barrier in the rat. *Invest Ophthalmol Vis Sci*. 1992;33:377–383.
18. Kumagai AK, Glasgow BJ, Pardridge WM. GLUT1 glucose transporter expression in the diabetic and nondiabetic human eye. *Invest Ophthalmol Vis Sci*. 1994;35:2887–2894.

19. Hosoya K, Sacki S, Terasaki T. Activation of carrier-mediated transport of L-cystine at the blood-brain and blood-retinal barriers in vivo. *Microvasc Res.* 2001;62:136–142.
20. Kuwabara T, Uchimura T, Takai K, Kobayashi H, Kobayashi S, Sugiyama Y. Saturable uptake of a recombinant human granulocyte colony-stimulating factor derivative, nartograstim, by the bone marrow and spleen of rats in vivo. *J Pharmacol Exp Ther.* 1995; 273:1114–1122.
21. Hosoya K, Tomi M, Ohtsuki S, et al. Conditionally immortalized retinal capillary endothelial cell lines (TR-iBRB) expressing differentiated endothelial cell functions derived from a transgenic rat. *Exp Eye Res.* 2001;72:163–172.
22. Hosoya K, Kondo T, Tomi M, Takanaga H, Ohtsuki S, Terasaki T. MCT1-mediated transport of L-lactic acid at the inner blood-retinal barrier: a possible route for delivery of monocarboxylic acid drugs to the retina. *Pharm Res.* 2001;18:1669–1676.
23. Tomi M, Hosoya K, Takanaga H, Ohtsuki S, Terasaki T. Induction of xCT gene expression and L-cystine transport activity by diethyl maleate at the inner blood-retinal barrier. *Invest Ophthalmol Vis Sci.* 2002;43:774–779.
24. Yamaoka K, Tanigawara Y, Nakagawa T, Uno T. A pharmacokinetic analysis program (MULTI) for microcomputer. *J Pharmacobiodyn.* 1981;4:879–885.
25. Wu X, Gutierrez MM, Giacomini KM. Further characterization of the sodium-dependent nucleoside transporter (N3) in choroids plexus from rabbit. *Biochim Biophys Acta.* 1994;1191:190–196.
26. Knott RM, Robertson M, Muckersie E, Forrester JV. Regulation of glucose transporters (GLUT-1 and GLUT-3) in human retinal endothelial cells. *Biochem J.* 1996;318:313–317.
27. Regina A, Roux F, Revest PA. Glucose transport in immortalized rat brain capillary endothelial cells in vitro: transport activity and GLUT1 expression. *Biochim Biophys Acta.* 1997;1335:135–143.
28. Sosula L, Beaumont P, Jonson KM, Hollows FC. Quantitative ultrastructure of capillaries in the rat retina. *Invest Ophthalmol Vis Sci.* 1972;11:916–925.
29. Boado RJ, Pardridge WM. A one-step procedure for isolation of poly(A)+ mRNA from isolated brain capillaries and endothelial cells in culture. *J Neurochem.* 1991;57:2136–2139.
30. Spector R, Johanson CE. The mammalian choroids plexus. *Sci Am.* 1989;261:48–54.
31. Root-Bernstein R, Busik JV, Henry DN. Are diabetic neuropathy, retinopathy and nephropathy caused by hypoglycemic exclusion of dehydroascorbate uptake by glucose transporters?. *J Theor Biol.* 2002;216:345–359.
32. Tang J, Zhu XW, Lust WD, Kern TS. Retina accumulates more glucose than does the embryologically similar cerebral cortex in diabetic rats. *Diabetologia.* 2000;43:1417–1423.
33. Bardr GA, Tang J, Ismail-Beigi F, Kern TS. Diabetes downregulates GLUT1 expression in the retina and its microvessels but not in the cerebral cortex or its microvessels. *Diabetes.* 2000;49:1016–1021.
34. Bode AM, Cunningham L, Rose RC. Spontaneous decay of oxidized ascorbic acid (dehydro-L-ascorbic acid) evaluated by high-pressure liquid chromatography. *Clin Chem.* 1990;36:1807–1809.
35. Ennis SR, Johnson JE, Pautler EL. In situ kinetics of glucose transport across the blood-retinal barrier in normal rats and rats with streptozocin-induced diabetes. *Invest Ophthalmol Vis Sci.* 1982; 23:447–456.
36. Mouithys-Mickalad A, Deby C, Deby-Dupont G, Lamy M. An electron spin resonance (ESR) study on the mechanism of ascorbyl radical production by metal-binding proteins. *Biometals.* 1998;11: 81–88.
37. Nualart FJ, Rivas CI, Montecinos VP, et al. Recycling of vitamin C by a bystander effect. *J Biol Chem.* 2003;278:10128–10133.
38. Kumagai AK, Vinorces SA, Pardridge WM. Pathological upregulation of inner blood-retinal barrier Glut1 glucose transporter expression in diabetes mellitus. *Brain Res.* 1996;706:313–317.
39. Huang J, Agus DB, Winfree CJ, et al. Dehydroascorbic acid, a blood-brain barrier transportable form of vitamin C, mediates potent cerebroprotection in experimental stroke. *Proc Natl Acad Sci USA.* 2001;98:11720–11724.
40. Bianchi J, Rose RC. Dehydroascorbic acid and cell membranes: possible disruptive effects. *Toxicology.* 1986;40:75–82.
41. Rose RC, Bode AM. Biology of free radical scavengers: an evaluation of ascorbate. *FASEB J.* 1993;7:1135–1142.

THE JOURNAL OF BIOLOGICAL CHEMISTRY
Vol. 279, No. 15, Issue of April 9, pp. 14835–14843, 2004
Printed in U.S.A.

SH2-containing Inositol Phosphatase 2 Predominantly Regulates Akt2, and Not Akt1, Phosphorylation at the Plasma Membrane in Response to Insulin in 3T3-L1 Adipocytes*

Received for publication, October 21, 2003, and in revised form, January 13, 2004
Published, JBC Papers in Press, January 26, 2004, DOI 10.1074/jbc.M311534200

Toshiyasu Sasaoka‡§¶, Tsutomu Wada§‖, Kazuhito Fukui‖, Shihou Murakami‖, Hajime Ishihara, Ryo Suzuki‡‡, Kazuyuki Tobe‡‡, Takashi Kadowaki‡‡, and Masashi Kobayashi‖**

*From the ‡Department of Clinical Pharmacology and ‖First Department of Internal Medicine, Toyama Medical and Pharmaceutical University, 2630 Sugitani, Toyama 930-0194, Japan, **Sainou Hospital, Toyama 930-0887, Japan, and ‡‡Department of Internal Medicine, Graduate School of Medicine, University of Tokyo, Tokyo 113-8655, Japan*

SH2-containing inositol phosphatase 2 (SHIP2) is a physiologically important negative regulator of insulin signaling by hydrolyzing the phosphatidylinositol (PI) 3-kinase product PI 3,4,5-trisphosphate in the target tissues of insulin. Targeted disruption of the SHIP2 gene in mice resulted in increased insulin sensitivity without affecting biological systems other than insulin signaling. Therefore, we investigated the molecular mechanisms by which SHIP2 specifically regulates insulin-induced metabolic signaling in 3T3-L1 adipocytes. Insulin-induced phosphorylation of Akt, one of the molecules downstream of PI3-kinase, was inhibited by expression of wild-type SHIP2, whereas it was increased by expression of 5′-phosphatase-defective (ΔIP) SHIP2 in whole cell lysates. The regulatory effect of SHIP2 was mainly seen in the plasma membrane (PM) and low density microsomes but not in the cytosol. In this regard, following insulin stimulation, a proportion of Akt2, and not Akt1, appeared to redistribute from the cytosol to the PM. Thus, insulin-induced phosphorylation of Akt2 at the PM was predominantly regulated by SHIP2, whereas the phosphorylation of Akt1 was only minimally affected. Interestingly, insulin also elicited a subcellular redistribution of both wild-type and ΔIP-SHIP2 from the cytosol to the PM. The degree of this redistribution was inhibited in part by pretreatment with PI3-kinase inhibitor. Although the expression of a constitutively active form of PI3-kinase myr-p110 also elicited a subcellular redistribution of SHIP2 to the PM, expression of SHIP2 appeared to affect the myr-p110-induced phosphorylation, and not the translocation, of Akt2. Furthermore, insulin-induced phosphorylation of Akt was effectively regulated by SHIP2 in embryonic fibroblasts derived from knockout mice lacking either insulin receptor substrate-1 or insulin receptor substrate-2. These results indicate that insulin specifically stimulates the redistribution of SHIP2 from the cytosol to the PM independent of 5′-phosphatase activity, thereby regulating the insulin-induced translocation and phosphorylation of Akt2 at the PM.

Phosphatidylinositol (PI)[1] 3-kinase plays a central role in the metabolic actions of insulin. PI(3,4,5)P_3 produced by activated PI3-kinase is thought to function as a key lipid second messenger for signaling to further downstream molecules including Akt and atypical PKC (1–4). We and others (5, 6) have recently cloned SH2-containing inositol phosphatase 2 (SHIP2), which has 5′-phosphatase activity toward the PI3-kinase product, PI(3,4,5)P_3, in the target tissues of insulin. Overexpression of SHIP2 inhibited insulin-induced metabolic signaling leading to glucose uptake and glycogen synthesis via 5′-phosphatase activity hydrolyzing the PI3-kinase product PI(3,4,5)P_3 to phosphatidylinositol 3,4-diphosphate in 3T3-L1 adipocytes and L6 myotubes (7, 8). Importantly, targeted disruption of the SHIP2 gene in mice increased insulin sensitivity without affecting other biological systems (9). These reports indicate that SHIP2 is a physiologically important negative regulator relatively specific to the insulin signaling. This prompted us to clarify the molecular mechanism by which SHIP2 specifically regulates the metabolic actions of insulin.

Among the effector molecules downstream of PI3-kinase, Akt is strongly implicated in the metabolic action of insulin including glucose uptake and glycogen synthesis (10–12). Upon insulin treatment, Akt is known to translocate from the cytosol to the plasma membrane where it is primarily activated by phosphorylation at $Thr^{308/309}$ and $Ser^{473/474}$ (13–16). Because Akt1 and Akt2 are the predominant isoforms expressed in 3T3-L1 adipocytes (17), the role of SHIP2 in the insulin-induced phosphorylation of Akt1 and Akt2 at various subcellular locations was examined by expressing the wild-type SHIP2 (WT-SHIP2) and a 5′-phosphatase-defective SHIP2 (ΔIP-SHIP2) into 3T3-L1 adipocytes using adenovirus-mediated gene transfer (7). Although PI3-kinase is activated by a number of growth factors, only insulin elicits the physiologically important metabolic action via the PI3-kinase pathway (18–20). In this regard, we investigated the impact of SHIP2 expression on the translocation and phosphorylation of Akt induced by the constitutively active form of PI3-kinase, myr-p110 (7, 21). Furthermore, to clarify whether SHIP2 specifically or non-specifically regulates the metabolic signaling of insulin mediated via IRS-1 and IRS-2, the effect of SHIP2 expression on the insulin-induced phosphorylation of Akt was studied in embryonic fibroblasts lacking either IRS-1 or IRS-2 (22). Here, we show that

* This work was supported in part by a grant-in-aid for Scientific Research from the Japan Society for the Promotion of Science (to T. S.). The costs of publication of this article were defrayed in part by the payment of page charges. This article must therefore be hereby marked "*advertisement*" in accordance with 18 U.S.C. Section 1734 solely to indicate this fact.

§ Contributed equally to this work.

¶ To whom correspondence should be addressed: Dept. of Clinical Pharmacology, Toyama Medical and Pharmaceutical University, 2630 Sugitani, Toyama 930-0194, Japan. Tel.: 81-76-434-7287; Fax: 81-76-434-5025; E-mail: tsasaoka-tym@umin.ac.jp.

[1] The abbreviations used are: PI, phosphatidylinositol; PI(3,4,5)P_3, PI 3,4,5-trisphosphate; PKC, protein kinase C; SHIP2, SH2-containing inositol phosphatase 2; WT, wild-type; PM, plasma membrane; DMEM, Dulbecco's modified Eagle's medium; FCS, fetal calf serum; m.o.i., multiplicity of infection; pfu, plaque-forming unit; LDM, low density microsomes; IRS, insulin receptor substrate.